Determination of N and O Atom Density in Ar-N 2-H 2 and Ar-O 2-H 2 Flowing Microwave Post Discharges

T. Czerwiec, J. Gavillet, T. Belmonte, H. Michel, André Ricard

Determination of N and O Atom Density in Ar-N_2-H_2 and Ar-O_2-H_2 Flowing Microwave Post Discharges

T. Czerwiec ([1,*]), J. Gavillet ([1]), T. Belmonte ([1]), H. Michel ([1]) and A. Ricard ([2])

([1]) Laboratoire de Science et Génie des Surfaces (**), Institut National Polytechnique de Lorraine, École des Mines de Nancy, parc de Saurupt, 54042 Nancy Cedex, France
([2]) Laboratoire de Physique des Gaz et des Plasmas (***), Université de Paris-sud, Bâtiment 212, 91405 Orsay, France

(Received 8 January 1996, revised 25 April 1996, accepted 3 June 1996)

PACS.52.70.Kz – Optical (ultraviolet, visible, infrared) measurements
PACS.82.40.Ra – Plasma reactions
PACS.82.40.Tc – Chemiluminescence and chemical laser kinetics

Abstract. — Number densities of N and O atoms have been determined using NO titration in Ar-N_2, Ar-N_2-H_2, Ar-O_2 and Ar-O_2-H_2 flowing microwave (2 450 MHz) post-discharges at 300 and 1500 Pa. The NO titration scheme is discussed from a kinetics point of view and applied to the high dilution of molecular gases in argon. The N/N_2 density ratio is enhanced by a factor 3 when small quantities of H_2 are introduced in Ar-N_2 discharges. The high O/O_2 density ratio obtained in Ar-O_2 post-discharges (0.5 to 0.6) are probably due to adsorbed H_2O that inhibits surface recombination of O-atom. The effect of H_2 addition in Ar-O_2 microwave discharge at 1500 Pa is to decrease the O atom density by homogeneous reaction involving H atoms and OH radicals.

1. Introduction

Flowing microwave post-discharges of reactive gases are studied for surface treatments without charged particles (electrons, ions) interactions. Such remote plasma processes have been performed in microelectronics to obtain Si_3N_4 and SiO_2 thin films [1,2] and in polymer treatments to increase the surface adhesion [3,4]. A flowing microwave post-discharge with N_2 and Ar-N_2 gas mixtures has been previously studied at high gas pressure ($5 \times 10^3 - 6.5 \times 10^4$ Pa) for steel surface nitriding [5]. The thickness and nitrogen content of γ' and ε iron nitride layers have been found to increase when a few H_2 was introduced into N_2 (Ar-N_2) to remove thin iron native oxide layers [6].

In the present work, the N atom density has been first determined by NO titration in Ar-N_2 and Ar-N_2-H_2 gas mixtures. Then, the O atom density has been deduced in Ar-O_2 and in Ar-O_2-H_2 gas mixtures by introducing NO in the post-discharge. Such a method, called the air-afterglow technique, has been previously proposed in oxygen post-discharge [7,8]. It is

(*) Author for correspondence (e-mail: czerwiec@mines.u-nancy.fr)
(**) Unité de Recherche associée au CNRS 1402
(***) Unité de Recherche associée au CNRS

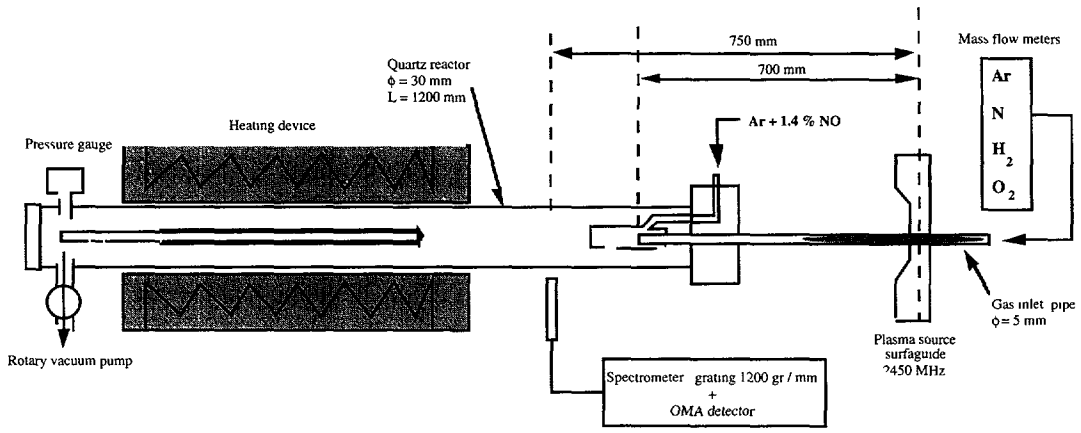

Fig. 1. — Experimental set-up for N and O atoms titration by NO.

presently extended to Ar-O_2-H_2 gas mixtures by taking into account the possible influence of the different gases on this titration scheme.

2. The Experimental Set-Up

The same flowing microwave post-discharge reactor as described in references [5,6] has been presently experimented. It is reproduced in Figure 1. The 2 450 MHz microwave plasma is produced in a quartz tube of 0.5 cm diameter with a surfaguide at a transmitted power of 130 W, a flow rate of 500-1050 sccm and a gas pressure of 300-1 500 Pa. The post-discharge runs into a reactor tube of diameter 2.8 cm at a distance of 70 cm from the surfaguide, corresponding to a post-discharge time $\Delta t \sim 10^{-2}$ s. Titration by NO is performed at the end of the 0.5 cm diameter quartz tube (75 cm from the surfaguide), in a mixing zone with a lateral exit of the flowing post-discharge (Fig. 1). The emission spectrum of the discharge and of the afterglow was analysed by using a Jobin-Yvon HR 640 spectrometer with a 1200 grooves mm^{-1} grating and a photodiode array detector (IRY/1024).

3. N-Atom Density in Ar-N_2 and Ar-N_2-H_2 Post-Discharges

The N-atom density has been previously determined by NO titration [5]. The following reactions occur:

$$N + NO \rightarrow N_2 + O \quad (a)$$
$$N + O + M \rightarrow NO(B) + M \quad (b)$$
$$NO(B) \rightarrow NO(X) + h\nu(NO_\beta)$$

at low NO flow rates and:

$$O + NO + M \rightarrow NO_2^* + M \quad (c)$$
$$NO_2^* \rightarrow NO_2 + h\nu \text{ (continuum)}$$
$$NO_2^* + M \rightarrow NO_2 + M \quad (d)$$

at high NO flow rates.

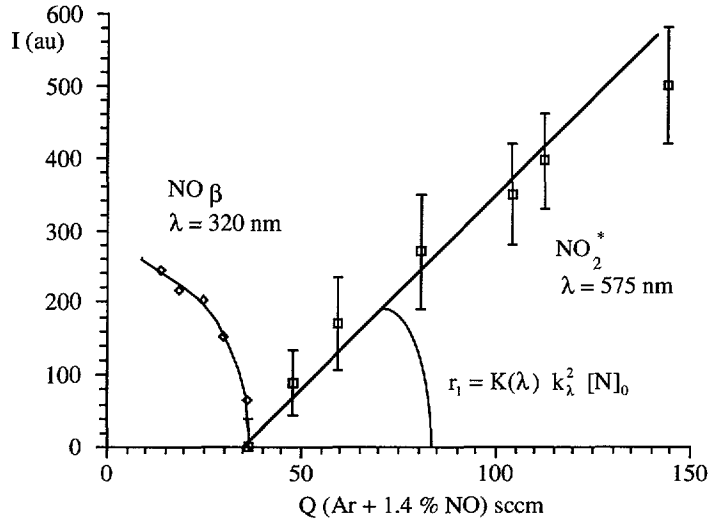

Fig. 2. — N-atom titration plot for an Ar-4% N_2 afterglow at P = 300 Pa, Q = 520 sccm and W = 130 W.

The colour change (extinction point) from the NO_β (violet) to the NO_2^* continuum (green) is produced as the two N and NO flow rates are equal in quantity. At this extinction point, all N-atom initially in the post-discharge have been converted into O-atom. The corresponding N-atom density $[N]_0$ can be written $[N]_0 = [O] = [NO]_{ext}$. By using an Ar-1.4% NO gas mixture, $[N]_0 = (7 \pm 0.4) \times 10^{13}$ cm^{-3} has been obtained as reproduced in Figure 2 for an Ar-4% N_2 post-discharge at 300 Pa. The total gas flow rate was Q = 520 sccm and the 2 450 MHz microwave power was W = 130 W. At 1 500 Pa of an Ar-5% N_2 post-discharge (Q = 1050 sccm) at the same HF power, it has been determined $[N]_0 = (4.1 \pm 0.1) \times 10^{14}$ cm^{-3} The $\frac{[N]}{[N_2]_i}$ density ratio (where $[N_2]_i$ denotes the density of N_2 with the discharge off), is 2.4% as for the experiment at 300 Pa. This relative density is calculated by assuming T = 300 K in the post-discharge.

The rate coefficients of reaction (a) - (d) are at T = 300 K: $k_a = 3.7 \times 10^{-11}$ cm^3 s^{-1} [9], $k_b^{Ar} = 0.8 \times k_b^{N_2}$ [10], $k_b^{N_2} = (2.4 - 3.1) \times 10^{-34}$ cm^6 s^{-1} [10,11], $k_c^{N_2} = 5.8 \times 10^{-32}$ cm^6 s^{-1}, $k_c^{Ar} = 3.7 \times 10^{-32}$ cm^6 s^{-1} and $k_c^{H_2} = 6 \times 10^{-32}$ cm^6 s^{-1} [12]. The radiative loss frequency of NO_2^* is $\gamma_r = 2.5 \times 10^4$ s^{-1} [13] and the quenching rate coefficients are $k_d^{Ar} = 3.9 \times 10^{-11}$ cm^3 s^{-1}, $k_d^{N_2} = 6 \times 10^{-11}$ cm^3 s^{-1} and $k_d^{H_2} = 7.3 \times 10^{-11}$ cm^3 s^{-1} [14].

In writing reactions (a) - (d), it has been neglected the effects of collisions on N_2 (X, v) and N_2 (A) metastable molecules. Such excited molecules could play an important part in the early afterglow by heating the remaining electrons by superelastic collisions [15] and by producing excitation transfers [16]. In the present condition of late afterglow, these processes have been neglected. However, the N_2(X, v) vibrational molecules are present with N-atom and can react with O-atom by:

$$N_2(X, v) + O \rightarrow NO + N \qquad (e)$$

The rate coefficient for reaction (e) is important for $v > 12$, $k_e(v > 12) = 10^{-11}$ cm^3 s^{-1} [17], but as reaction (e) is followed by reaction (a) to restore O-atom, it has no effect on the presented kinetic schemes.

After the extinction point (for $[NO] > [NO]_{ext}$), the NO_2^* density is linearly increasing with [NO] as shown in Figure 2. Such a variation can be explained by the following kinetics relation:

$$[NO_2^*] = \frac{[O][NO][M]k_c^M}{\gamma_r + [M]k_d^M} \tag{1}$$

By writing equation (1), the following two bodies reaction:

$$O + NO \rightarrow NO_2^* \tag{f}$$

with $k_f = 5.6 \times 10^{-17}$ cm^3 s^{-1} [18] has been neglected for gas pressure $P > 100$ Pa, since $[M]k_c^M > 2 \times 10^{-16}$ cm^3 s^{-1} for M = Ar. The radiative frequency γ_r can be neglected in equation (1) for $P > 100$ Pa since $[M]k_d^M > 10^6$ s^{-1} for M = Ar. Then, for high dilution of N_2 and H_2 molecular gases into argon, the intensity $I(NO_2^*)$ of the air afterglow continuum can be described by equation (2) in an Ar-N_2 gas mixture and by equation (3) in an Ar-N_2-H_2 gas mixture:

$$I(NO_2^*) = K(\lambda)[O][NO] = K(\lambda)[N]_0[NO] \tag{2}$$

$$I(NO_2^*) = K(\lambda)[N]_0^{H_2}[NO] \tag{3}$$

with

$$K(\lambda) = k(\lambda)\frac{\sum_M k_c^M[M]}{\sum_M k_d^M[M]} \approx \frac{k_c^{Ar}}{k_d^M}k(\lambda) = 9.5 \times 10^{-22}k(\lambda) \tag{4}$$

$k(\lambda)$ is a calibration factor depending on spectrometer spectral response, on photon energy and optical emission probability of NO_2^* and $[N]_0^{H_2}$ is the initial N-atom density in the Ar-N_2-H_2 gas mixture. Note that chimiluminescence with O_3 has not been considered here since, first substantial O_3 density only appears at high O_2 gas pressure and second, the NO-O_3 continuum is extending from 600 to 2200 nm [18] at larger wavelengths that presently used for NO_2^* detection: $\lambda = 575$ nm.

The results obtained with an Ar-3.8% N_2-0.2% H_2 gas mixture at $P = 300$ Pa, $Q = 521$ sccm and $W = 130$ W are reproduced in Figure 3. First, it is found a sensitive increase of N-atom density with $[N]_0^{H_2} = (2.3 \pm 0.1) \times 10^{14}$ cm^{-3} which is 3.3 higher than without H_2. The increase of N-atom density with a few H_2 into N_2 has been previously analysed by LIF in DC N_2-H_2 flowing post-discharge [19]. Recently, an increase of about 3 of N-atom density has been found in an Ar-10% N_2-0.5% H_2 microwave post-discharge [20]. This seems to be connected to an increase of the discharge electric field and to a reduction of N-atom recombination on the post-discharge tube as a few H_2 is introduced into N_2.

The slope of the I (NO_2^*) variations with NO as determined in Figures 2 and 3 are $r_1 = K(\lambda)[N]_0$ and $r_2 = K(\lambda)[N]_0^{H_2}$, respectively. With $r_1 = 5.3 \pm 0.9$, $[N]_0 = (7 \pm 0.4) \times 10^{13}$ cm^{-3}, $r_2 = 16 \pm 2$ and $[N]_0^{H_2} = (2.3 \pm 0.1) \times 10^{14}$ cm^{-3}, it follows that:

$$\frac{r_2}{r_1} = \frac{[N]_0^{H_2}}{[N]_0} \tag{5}$$

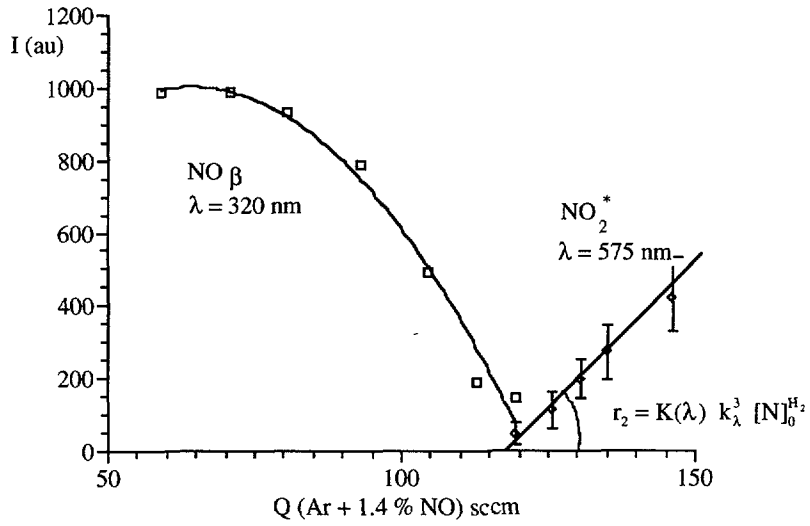

Fig. 3. — N-atom titration plot for an Ar-3.8% N_2-0.2% H_2 afterglow at $P = 300$ Pa, $Q = 521$ sccm and $W = 130$ W.

4. O-Atom Density in Ar-O_2 and in Ar-O_2-H_2 Post-Discharges

In Ar-O_2-H_2 post-discharge, the oxygen atoms coming from the discharge are reacting with NO to produce NO_2^* by reaction (c). For high O_2 and H_2 molecular gases dilution into argon and by using the following rate coefficients in equation (4): $k_c^{O_2} = 5.6 \times 10^{-32}$ cm^{-6} s^{-1} [12] for reaction (c) and $k_d^{O_2} = 5.4 \times 10^{-11}$ cm^3 s^{-1} [14] for reaction (d), it can be deduced that:

$$I(NO_2^*) = K(\lambda)[O][NO] \tag{6}$$

Variation of NO_2^* intensity *versus* NO measured at the same wavelength with the same optical arrangement as above is reproduced in Figure 4 for an Ar-3.8% O_2-0.2% H_2 post-discharge at $P = 300$ Pa, $Q = 521$ sccm and $W = 130$ W. At this low H_2 percentage, the contribution of possible H_2O formed in the post-discharge has been neglected. The slope of NO_2^* intensity *versus* Ar-1.4% NO flow rate is $r_3 = K(\lambda)[O]$ and by comparing with Figure 2 and Figure 3, it follows:

$$[O] = \frac{r_3}{r_1}[N]_0 = \frac{r_3}{r_2}[N]_0^{H_2} \tag{7}$$

With $r_3 = 120 \pm 10$, $r_1 = 5.3 \pm 0.9$, $[N]_0 = (7 \pm 0.4) \times 10^{13}$ cm^{-3}, equation (6) gives $[O] = (1.6 \pm 0.5) \times 10^{15}$ cm^{-3}. It results that the density ratio $C_0 = \frac{[O]}{[O_2]_i}$ (where $[O_2]_i$ denotes the density of O_2 with the discharge off) in the actual Ar-3.8% O_2-0.2% H_2 flowing HF post-discharge at 300 Pa is as high as 0.6. This value is considerably higher than those obtained in pure oxygen microwave post-discharges which normally ranges around 0.01 and 0.1 [21–24] and could only compared to C_0 obtained in microwave discharge in O_2 [25]. Such high O atom density is probably due to the high argon dilution used in the present experiments and to the use of hydrogen.

It has been previously found that small amounts of molecular gases (N_2, H_2) increase the extent of dissociation of O_2 molecules in electrical discharges [22, 23]. In a microwave post-discharge at 70 Pa, Brown [22] observed an increase in C_0 up to 0.5 when traces of impurities

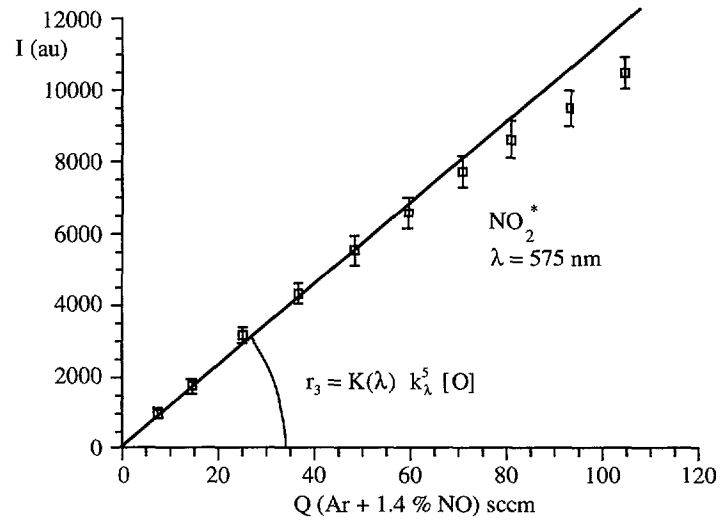

Fig. 4. — O-atom titration plot for an Ar-3.8% O_2-0.2% H_2 afterglow at $P = 300$ Pa, $Q = 521$ sccm and $W = 130$ W.

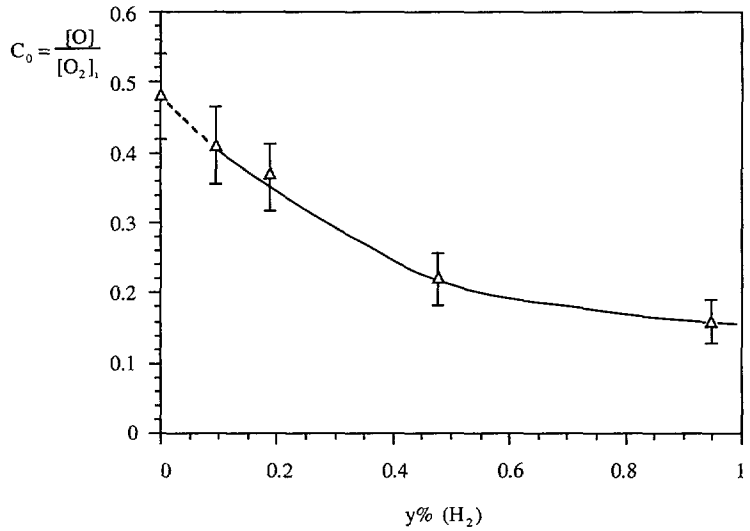

Fig. 5. — Relative O-atom density (C_0) *versus* hydrogen percentage (y %) for an Ar-1.2% O_2-y % H_2 microwave discharge at $P = 1\ 500$ Pa, $1\ 039.5 \leq Q \leq 1\ 049.5$ sccm and $W = 130$ W.

such H_2O or H_2 were injected in the O_2 discharge. As it is reproduced in Figure 5 for the present experiment at 1 500 Pa ($1\ 039.5 \leq Q \leq 1\ 049.5$ sccm), the oxygen atom density in the Ar-1.2% O_2-y% H_2 post-discharge is decreasing from $[O] = (2.1 \pm 0.4) \times 10^{15}$ cm^{-3}, $C_0 = 0.48$ as $y(H_2) = 0$ to $(7 \pm 1) \times 10^{14}$ cm^{-3}, $C_0 = 0.16$ as $y(H_2) = 1\%$. This behaviour was also observed by increasing the pressure at constant mass flow rate and constant H_2 addition in O_2 [22]. The high initial C_0 value may be due to impurities such as water vapour adsorbed on the reactor

walls [28]. Moreover, the destruction of O atoms may be either by heterogeneous (surface recombination) or by homogeneous (gas phase) reactions. The decrease of O-atom density in introducing H_2 in the high pressure Ar-O_2 gas mixture could be explained by homogeneous reaction involving H atoms and OH radicals such as:

$$O + H + M \rightarrow OH + M \quad (g)$$
$$O + OH \rightarrow O_2 + H \quad (h)$$

with $k_g = 4.3 \times 10^{-32}$ cm^6 s^{-1} [26] and $k_h = 2.9 \times 10^{-11}$ cm^3 s^{-1} [27].

5. Conclusion

The O-atom density determination by NO titration has been discussed from kinetic point of view for the complex post-discharge in Ar-O_2-H_2. Addition of small quantities of H_2 to Ar-N_2 mixture has been investigated for N-atom density determination and consequences on O-atom density determination is also discussed. It can be concluded that N-atom density is significantly enhanced by H_2 addition by a factor 3 in Ar-3.8% N_2-0.2% H_2 at 300 Pa (Q = 520 sccm). Both Ar-N_2 and Ar-N_2-H_2 mixtures can serve as references for O atom titration by NO in Ar-O_2 or Ar-O_2-H_2 post-discharge. Relative O-atom densities as high than 0.5-0.6 has been determined in Ar-O_2 post-discharge at 300 Pa (Q = 520 sccm) and 1 500 Pa (Q = 1 039.5 sccm). This is probably related to H_2O settled on the reactor walls that inhibits the surface recombination of O-atom. It has been found a sensitive decrease of O-atom density as H_2 is initially introduced in an Ar-O_2 gas mixture. Works are in progress to analyse the kinetics processes in Ar-O_2-H_2 gas flowing post-discharges.

Acknowledgments

The authors wish to express their thanks to J.P. Prelot for his technical support.

References

[1] Kulisch W., Remote plasma-enhanced chemical vapour deposition with metal organic sources gases: principles and applications, *Surf. Coat. Technol.* **59** (1993) 193.
[2] Tsu D.V., Parsons G.N., Lucovsky G. and Watkins M.W., Optical emission and mass spectrocopic studies of the gas phase during the deposition of SiO_2 and a-Si: H remote plasma-enhanced chemical vapour deposition, *J. Vac. Sci. Technol. A* **7** (1989) 1115.
[3] Normand F., Marec J., Leprince Ph. and Granier A., Surface treatment of polypropylene by oxygen microwave discharge, *Mat. Sci. Engn. A* **139** (1991) 103.
[4] Normand F., Granier A., Leprince Ph., Marec J., Shi M.K. and Clouet F., Polymer treatment in the flowing afterglow of an O_2 microwave discharge, *Plasma Chem. Plasma Proc.* **15** (1995) 173.
[5] Ricard A., Oseguera-Pena J., Falk L., Michel H. and Gantois M., Active species in microwave post-discharge for steel-nitriding, *IEEE Trans. Plasma Sc.* **18** (1990) 940.
[6] Malvos H., Michel H. and Ricard A., Correlation between active species density and iron nitride layer in Ar-N_2-H_2 microwave post-discharge, *J. Phys. D* **27** (1994) 1328.
[7] Clyne M.A.A. and Nip W.S., Reactive Intermediates in the gas phase, D.W. Setser Ed. (Academic Press, 1979).

[8] Piper L.G., Caledonia G.E. and Kennealy J.P., Rate constants for deactivation of N_2 ($A^3\Sigma_u^+, v' = 0, 1$) by O, *J. Chem. Phys.* **75** (1981) 2847.

[9] Michael J.V. and Lim K.P., Rate constants for the N_2O reaction system: thermal decomposition of N_2O; $N + NO \rightarrow N_2 + O$; implication for the $O + N_2 \rightarrow NO + N$, *J. Chem. Phys.* **97** (1992) 3228.

[10] Baulch D.L., Drysdale D.D. and Horne D.G., Homogeneous gas phase reactions of a H_2, N_2, O_2 system (London Butterworths, 1973).

[11] Gross R.W.F. and Cohen N., Temperature dependence of chimiluminescent reactions. II Nitric oxide afterglow, *J. Chem. Phys.* **48** (1968) 2582.

[12] Young R.A., Black G. and Slanger T.G., Reaction and deactivation of O (1D), *J. Chem. Phys.* **49** (1968) 4758.

[13] Hakala D.F. and Reeves R.R., Ruby laser induced emission from NO_2, *Chem. Phys. Lett.* **32** (1976) 510.

[14] Donnely V.M., Keil D.G. and Kaufman F., Fluorescence lifetime studies of NO_2. III Mechanisms of fluorescence quenching, *J. Chem. Phys.* **71** (1979) 659.

[15] Colonna G., Gorse G., Capitelli M., Winkler R. and Wilhelm J., The influence of electron-electron collisions on electron energy distribution functions in N_2 post-discharge, *Chem. Phys. Lett.* **213** (1993) 5.

[16] de Benedictis S., Dilacce G. and Simek M., Time resolved LIF spectroscopy on N_2 (A) metastable in a He/N_2 pulsed RF discharge, *Chem. Phys.* **178** (1993) 547.

[17] Gordiets B. and Ricard A., Production of N, O and NO in N_2-O_2 flowing discharges, *Plasma Sources Sci. Technol.* **2** (1993) 158.

[18] Sutoh M., Morioka Y. and Nakamura M., Absolute rate constant for the chimiluminescent reactions of atomic oxygen with nitric oxide, *J. Chem. Phys.* **72** (1980) 20.

[19] Amorim J. , Baravian G. and Ricard A., Production of N, H and NH active species in N_2-H_2 dc flowing discharges, *Plasma Chem. Plasma Proc.* **15** (1995) 723.

[20] Bockel S., Amorim J., Baravian G., Ricard A. and Stratil P., Spectroscopic study of active species in dc and hf flowing discharges in N_2-H_2 and Ar-N_2-H_2 mixtures, *Plasma Sources Sci. Technol.* (1996) to be published.

[21] Granier A., Pasquiers S., Boisse-Laporte C., Darchicourt R., Leprince P. and Marec J., Characterization of a low pressure oxygen discharge created by surface waves, *J. Phys. D* **22** (1989) 1487.

[22] Brown R.L., Effects of impurities on the production of oxygen atoms by microwave discharge, *J. Phys. Chem.* **71** (1967) 2492.

[23] Mearns A.M. and Morris A.J., Use of the nitrogen dioxide titration technique for oxygen atom determination at pressures above 2 Torr, *Chem. Eng. Symp. Ser.* **112** (1971) 37.

[24] Kaufman F. and Kelso J.R., Catalytic effects in the dissociation of oxygen in microwave discharges, *J. Chem. Phys.* **32** (1960) 301.

[25] Brake M., Hinkle J., Asmussen J., Hawley M. and Kerber R., Dissociation and recombination of oxygen atoms produced in a microwave discharge, *Plasma Chem. Plasma Proc.* **3** (1983) 63.

[26] Tsang W. and Hampson R.F., Chemical kinetic data base for combustion chemistry, Part. I: Methane and related compounds, *J. Phys. Chem. Ref. Data* **15** (1986) 1087.

[27] Baulch D.L., Cobos C.J., Cox R.A., Frank P., Hayman G., Just Th., Kerr J.A., Murrells T., Pilling M.J., Troe J., Walker R.W. and Warnatz J., Summary table of evaluated kinetic data for combustion modelling, *Combust. Flame* **98** (1994) 59.

[28] Collart E.J.H., Baggerman J.A.G. and Visser R.J., On the role of atomic oxygen in the etching of organic polymers in a radio-frequency oxygen discharge, *J. Appl. Phys.* **78** (1995) 47.